Journal of Material Cycles and Waste Management (2020) 22:1434-1443
https://doi.org/10.1007/s10163-020-01032-3

ORIGINAL ARTICLE

Preparation and properties of fly ash-based geopolymer concrete with alkaline waste water obtained from foundry sand regeneration process

S M Fuad Kabir Moni[1] · O. Ikeora[1] · C. Pritzel[1] · B. Görtz[1] · R. Trettin[1]

Received: 14 May 2019 / Accepted: 1 April 2020
© The Author(s) 2020, corrected publication 2021

Abstract
The aim of the research was to investigate the influences of high alkaline content foundry sand regeneration wastes incorporated with fly ash in the production of geopolymer concrete. The fly ash-based geopolymer concrete was activated using alkaline solutions of sodium silicate and sodium hydroxide. The geopolymeric products were characterized using X-ray diffraction, scanning electron microscopy, Fourier-transform infrared spectroscopy and simultaneous thermal analysis. A higher compressive strength was observed in mechanical strengths test in the geopolymer and its respective foam concrete made of waste water in comparing to reference water (tap water). Furthermore, a packed arrangement and lower pore size distribution for both geopolymer and foam concrete were observed using nitrogen gas adsorption and mercury intrusion porosimetry, in contrast, to waste water and reference water.

Keywords Geopolymers · Alkaline activator · Curing temperature · Foam geopolymer concrete · Waste water · Fly ash

Introduction

High demand for environment-friendly construction materials has been the key challenge for the scientist in recent years [1]. The production of cement consumes energy and also emits greenhouse gases which have adverse impacts on the environment. Davidovits [2] reported that the production of about one ton of Portland cement results in the emission of one ton of carbon dioxide (CO_2) which varies with the technique used in the production process. The cement industry is the largest producer of CO_2 in the world, due to a large amount of produced concrete (over 1 billion tons a year worldwide [1]). Partial replacement of cement using supplementary cementitious materials (SCMs) has been discovered with the aim of providing solutions towards reducing the dependency on cement. The effect was high compared to a 100% replacement of cement by a very low CO_2 emission geopolymer [3]. McCaffrey [4] reported that generated CO_2 emissions by the cement industries can be reduced by limiting the amount of calcined material in cement. This can only be done by decreasing the amount of cement in concrete which will result in a decrease in the number of constructions dependent on cement compared to construction with others. A number of studies [5, 6] reported that the amount of CO_2 emission generated from the production of geopolymers is about 60–80% less than the cement clinker. Geopolymers are in an inorganic polymeric structure formed by alkaline activation of raw materials containing silica and alumina [7]. The silica and alumina coming from materials like fly ash, granulated cortex slag, granulated blast furnace slag, volcanic ash, palm oil fuel ash, red mud, blast furnace slag, metakaolin, and kaolinite. These silicon and aluminum oxides can be activated by the reaction of the aluminosilicate with alkaline solutions of alkali metal hydroxide and alkali metal silicate [8]. Alkaline activating agents widely used in the formation of geopolymers are the mixture of sodium or potassium hydroxide (NaOH, KOH) and sodium silicate or potassium silicate (Na_2SiO_3, K_2SiO_3) [9, 10]. However, sodium-based activating agents are preferably used due to their lower cost compared to potassium-based activating agents.

The term ‘alkaline activation’ describes the fast polymerization reaction of the alumina-silicate present in the mentioned raw materials with the alkaline solution of NaOH and

✉ S M Fuad Kabir Moni
kabir@chemie.uni-siegen.de

[1] Institute for Building and Materials Chemistry, University of Siegen, Paul Bonatz Str. 9–11, 57068 Siegen, Germany

Na_2SiO_3 to yield a three-dimensional polymeric chain and a ring structure consisting of Si–O–Al–O bonds [11]. Geopolymers cause the formation of polymeric Si–O–Al bonds for strength and compactness while the cement-based concrete enables the formation of calcium-silicate hydrates for matrix formation and mechanical strength [12]. These hydration products found in both geopolymer and cement-based concrete are responsible for dense matrix formation in their microstructure. A number of parameters play roles in the formation of favorable properties on the polymerized products. This parameter depends on raw material, type of water used, curing time and temperature, type of alkaline activators and alkaline solution concentrations. They give direct influences on the mechanical strength, shrinkage, microstructure and other physical properties of the polymerized products [13]. Rangan [14] suggested that the optimum curing temperature is 60 °C which gives the highest compressive strength in geopolymer concrete. A number of advantages that geopolymer concrete has over cement-based concrete include fire retardant, greater resistance to acid and sulfate attacks, resistance to high temperatures, high early strength, little or no water required and high mechanical strength [15–17]. Some researchers [18, 19] suggested that the compressive strength of concrete formed with foundry sand was higher than the similar mix with the same quality fresh sand. This indicates the reusability of foundry sand for concrete production. On the other hand, sand with added binders is used as a mold in the foundry industry. The regeneration of molded sand is very important for the foundry industry because it reduces the demand for new sand and cost for the industry. The wet regeneration can be used to remove water-soluble binders like a water glass. Furthermore, the reduction of this high alkaline waste water is a very important factor, since the disposal of waste is expensive. This wet process proceeds as follows; at first, the molded sand is pre-heated and then water is added to wash the sand by an external force (mechanical mixer). Afterward, the slurry (water and sand) is rinsed with water to remove the water glass from the sand. Finally, at the last steps, the sand is dewatered (waste water) and dried for further application. The waste water containing Na_2SiO_3 is used for the utilization of the geopolymer system to give an extra activator for the aluminosilicate materials.

Research consequence

To date, geopolymer concretes have been studied with different analytical methods to determine the geopolymerization and strength using one type of fly ash, foundry used sand, corresponding new sand and waste water from foundry sand regeneration process in each study using a unique mixing procedure technique. This research reports the geopolymer concrete and its corresponding foam concrete performance up to 6 days using a Class F fly ashes with the same mixing process. It provides a systematic study of microstructures and strength for a range of geopolymer concretes. Thus, the reported geopolymer research data give a clear perceptive of this novel concrete's performance, made with the wide range of low-calcium fly ash representative of those that exist throughout the world.

Materials and methods

Materials

The fly ash (Class F, ASTM C-618) as EFA-Füller® from BauMineral GmbH (Herten, Germany), was used as the aluminosilicate source material in the production of the geopolymer concretes (see composition on Table 1). The chemical compositions of new sand (H31, Quarzwerke GmbH, Frechen, Germany) and used sand (after applied binder to make mold for aluminum casting) are also shown in Table 1. A pellet of sodium hydroxide obtained from CHEMSOLUTE (Renningen, Germany) was used to make NaOH solution. Sodium silicate (Na_2SiO_3) was purchased from Carl Roth GmbH & Co. KG. The foaming agent, TEGO Betain F 50 which was used in the preparation of the foam geopolymer was received from Evonik Industries AG (Essen, Germany). The reference water used was laboratory tap water (pH = 8) and the waste water (pH = 10.2) had been obtained from laboratory-based wet regeneration process of foundry molded sand.

Table 1 Chemical composition of class F Fly ash, used sand and corresponding new sand in (weight %) via XRF

Oxides	Na_2O	Al_2O_3	SiO_2	Fe_2O_3	Mn_2O_3	MgO	K_2O	CaO	Cr_2O_3	P_2O_5	TiO_2	ZrO_2	SO_3	LOI
Fly ash (FA)	0.69	25.4	53.3	6.49	0.078	2.10	1.6	6.4	0.015	1.37	1.29	0.084	–	2.24
New sand	0.17	0.28	99.1	0.14	< 0.01	0.26	0.042	0.26	< 0.01	–	0.029	–	0.043	0.09
Used sand	0.21	0.11	99.5	0.035	< 0.01	< 0.01	0.061	< 0.01	< 0.01	–	0.032	–	0.056	0.33

Specimen preparation

Mixing of geopolymer paste with and without foam

The mass ratio of 0.23 was used for NaOH to Na_2SiO_3. Prior to making the paste 1-min dry mixing of the solids was performed. Afterward, the alkaline solutions along with water were added and mixed for further 9 min (possible similar consistency for all sample) and finally poured into a (160 mm × 40 mm × 40 mm) mold consisting of three columns of equal dimensions. To make the foam the foaming agent and water based on a mass ratio of 0.008 was taken (which was previously optimized for mass ratio with mixing time) and stirred continuously using a mixer (as a foam creator, Hobart N50) for 3.5 min to obtain the stabilized foam. An amount of 20 vol% of the geopolymers concrete stone (taking arbitrary, introducing possible 20% more pore in that system) was used for all foam geopolymers concrete stone. The resulting foam was added to the geopolymer paste and stirred for an additional 5 min followed by casting of the foamed concrete into a prism mold (geopolymers concrete stone) and curing. The optimized mix design of the geopolymers concrete stone (with and without foam) is shown in Table 2.

Curing time and temperature

All samples were left at room temperature 20 ± 2 °C for 3 days (for initial hardening) followed by curing at 60 ± 5 °C for additional 3 days (for final hardening) in an oven. After 6 days, the specimens were de-molded (geopolymers concrete stone), afterward, the characterization of samples was conducted. Table 3 shows the designation of the investigated samples. The sample GP05 and GP06 were used as a reference for the without and with foam respectively to compare to other specimens.

Testing procedures and equipment

The isothermal heat calorimetric analysis [DCA, Toni CalHexa (Toni Technik Baustoffprüfsysteme GmbH)] was used to check the reactivity of fly ash with respect to different molar solutions of NaOH. The solid to the liquid ratio of 0.5 was used in the experiment. The composition analysis of polymerization products was done by XRD [X'Pert PRO diffractometer (PANalytical B.V)], FTIR [Tensor 27, Bruker] and STA (Simultaneous Thermal Analysis) [STA 449 C Jupiter (Netzsch Group)]. Furthermore, microstructure analysis of polymerization products was conducted using SEM [ESEM Quanta 250 FEG (FEI Deutschland GmbH)] and EDX [EDAX Inc. (DET_APOLLO_XL)]. Images of the foam morphology were obtained using a digital camera [Canon PowerShot A3500 (16MP)]. The pore size distribution and the specific surface area were obtained by N_2 gas adsorption [Micromeritics ASAP2020 (Micromeritics GmbH)] and MIP (Mercury Intrusion Porosimetry) [AutoPore IV (Micromeritics GmbH)]. Compressive and flexural strength tests of prepared geopolymer stones were performed using the strength testing device [TONI TECHNIK, TONI COMP III]. The liquid phase quantitative analysis of possible existed anion and cation in the waste and tap water were performed by IC [(Ion Chromatography, Dionex DX-100 (cation) and ICS-1100 (anion)]. The chemical composition of the finely grounded, fly ash, sand and solid residue of waste water was analyzed by means of X-ray fluorescence analysis (XRF) [HuK Umweltlabor GmbH, Germany].

Table 2 Optimized mix design of the geopolymer concrete stone (with and without foam)

Materials used	Weight (g)
Fly ash	250.00
Coarse sand	292.40
Fine sand	315.25
NaOH (aq)	26.40
Na_2SiO_3	113.50
Water	80.00
Foaming agent	0.88
Water for foam	99.12

Table 3 Designation of the investigated samples

Sample number	Geopolymer concrete samples
GP02	Waste water concrete with used foundry sand
GP03	Corresponding foam (20% vol.) concrete of GP01
GP04	Corresponding foam (20% vol.) concrete of GP02
GP05	Tap water concrete with new sand
GP06	Corresponding foam (20% vol.) concrete of GP05

Results and discussion

Characterization of waste water

The number of anions and cations present in the waste and tap water were obtained using ion chromatography and shown in Table 4. The analysis indicates that the waste water has a high quantity of sodium followed by potassium, calcium, and magnesium with respect to cations. In the anions part, phosphate, sulfate and chloride ions were observed in quantities of 149, 49.1 and 36.6 mg/L respectively. The significant amount of the sodium content is coming from the sodium water glass which is used as the binder for the molding purpose in the foundry industries. This significant sodium content can give an extra activator on the polymerization of the geopolymer stone. The considerable amounts

Table 4 Ion concentration of anions and cations present in tap water and waste water measured by ion chromatography

Anions	Concentration (mg/L)		Cations	Concentration (mg/L)	
	Tap water	Waste water		Tap water	Waste water
Fluoride	0.05	1.80	Lithium	–	1.39
Chloride	0.10	36.60	Sodium	7.70	**913.26**
Nitrate	4.60	3.70	Ammonium	< 0.05	0.46
Phosphate	0.06	**149.00**	Potassium	0.81	75.73
sulfate	13.00	49.10	Magnesium	4.60	10.00
–	–	–	Calcium	23.00	22.79

Table 5 Analytical compositions of the solid residue of the waste water determined by EDX and XRF (weight %)

	C	O	Na	Al	Si	P	S	Cl	K	Ca
EDX results	12.1	41.9	21.7	0.7	12.9	6.5	0.3	0.2	2.1	1.5
	C	CO_2	Na_2O	Al_2O_3	SiO_2	P_2O_5	SO_3	Cl^-	K_2O	CaO
XRF results	7.4	17.1	29.3	1.4	27.8	11.6	0.6	0.2	2.5	2.2

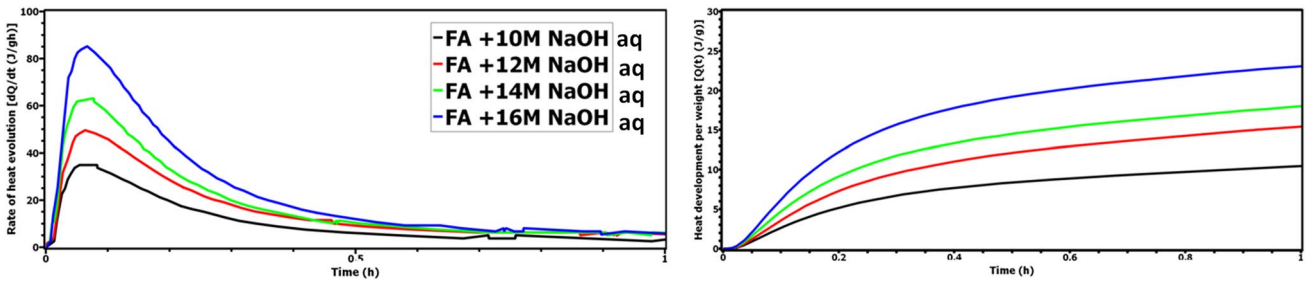

Fig. 1 Isothermal plot of heat evolution (left) and development (right) in the reaction of fly ash (FA) and NaOH solution over time

of phosphate also help in polymerization, as the phosphate has the ability to form inorganic polymers [2].

Table 5 highlights the percentage of the elements and oxide compounds in the solid residue (tap water does not contain significant solid after filtering (589 Schwarzband, 125 mm, Ref. No.300 011) in same procedure as waste water) of the waste water (which containing 1.15 wt% analyzed by normal gravity filtration process) as analyzed by EDX and XRF methods. Good consistency is confirmed in the results between EDX and XRF analysis.

Waste water in geopolymerization

The study of the reactivity of fly ash and NaOH was carried out using DCA. The heat evolved during this reaction was determined as a function of time.Figure 1 shows that an increase in the concentration of NaOH leads to increased interaction with fly ash. High concentrations of NaOH lead to the faster dissolution of the solid materials and increase the polymerization reaction which affects the compressive

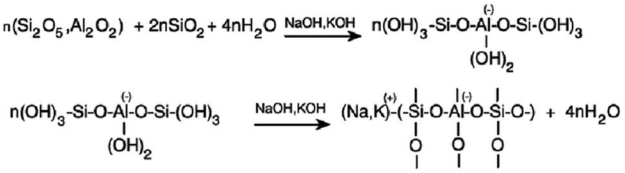

Fig. 2 The general reaction equation for geopolymer formation [2]

strength. The schematic diagram of the general reaction for the formation of geopolymer [2] is shown in Fig. 2**.**

The increase in compressive strength resulting from an increase in the concentration of NaOH was largely due to the intense leaching of silica and alumina from fly ash [20]. From Fig. 1, the optimum reactivity, that is, the largest heat evolution was observed for the concentration of 16 M NaOH and it was selected and utilized throughout the whole investigations.

The polymerized products and educts (fly ash) are in amorphous nature [11] and the amorphous or nano-crystalline nature phases are difficult to be identified by XRD

but the knowledge of the polymeric reaction which occurs upon activation provides insight on some of these phases [11, 12]. Therefore, the phase constituents of each geopolymer concrete and foam concrete were examined using the XRD equipment as shown in Fig. 3. However, striking similarities were observed in the XRD analysis of all samples. Sharp peaks of crystalline phases comprising of mullite ($Al_6Si_2O_{13}$) and quartz (SiO_2) were identified. The literature [21, 22] suggested that these crystalline phases of mullite and quartz were also present in fly ash and geopolymer concrete. The intensity of the peaks depends on the crystallization of the phases, which may be attributed to the age of curing on the geopolymers.

Figure 4 shows the combined results of the characteristic bands from FTIR, for a geopolymer example with fly ash, the usual infrared spectrum of this type of materials is characterized by different types of bands. The most attribute band is located between 900 and 1100 cm^{-1}, which is important in these studies, and it is attributed to the asymmetric stretching "X-O" (where X represents to Si or Al) and is the one of the asymmetric stretching present in the gel of hydrated sodium aluminosilicate. The extent of this band is mainly credited to the amorphous nature of the material, as well as the short-range ordering of SiO_4 and AlO_4 tetrahedron. Moreover, this graph also allows us to deduce the degree of transmittance in the band and which depends on factors such as the cured age or the degree of reactivity, among others [23, 24]. Also, these materials tend to report small bands located between 600 and 650 cm^{-1} and bands between 790 and 800 cm^{-1}, which are attributed to the bonds present in the fly ash source (quartz and mullite) [24].

Simultaneous thermal analysis (STA) consists of thermogravimetric (TG) and differential scanning calorimetric (DSC), which give information on the mass loss of the sample due to decomposition of the compounds present in it and phase changes associated with the heat release or absorption by the sample under a temperature-controlled environment.

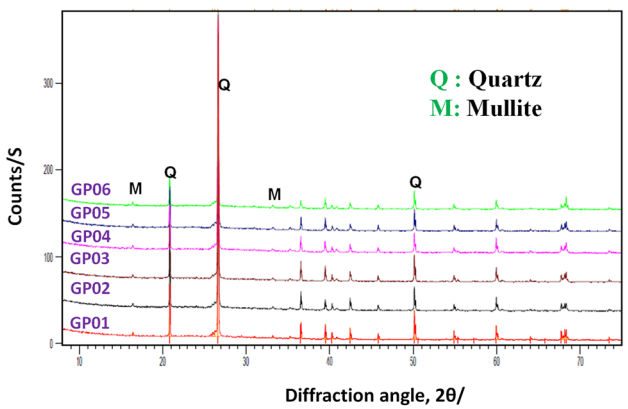

Fig. 3 XRD patterns of the geopolymer stones

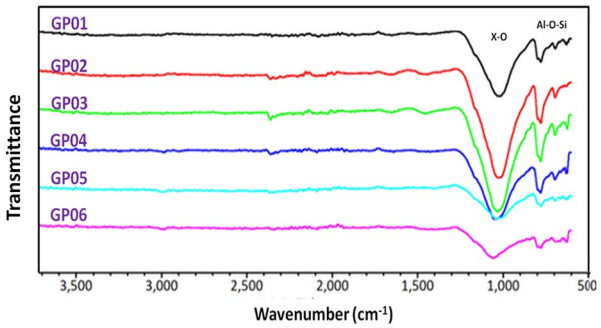

Fig. 4 FTIR spectra of the geopolymer stones

In Fig. 5, TG curves from 0 to 1000 °C indicate the loss of water from the hydrated gels. Hardened geopolymers contain three types of water, which were removed during TG analysis with respect to temperature (see Table 6).

Within the range of 0–100 °C, larger mass losses in physically bonded water are noticed for GP03 and GP04 and this is due to the foam geopolymer concrete. In addition, the GP04 showed more mass loss in the range of 101–300 °C (chemically bonded water) and 301–1000 °C (polycondensation of bond S–O–Si) compared to GP03, which is the indication of higher polymerization products. The DSC curves showed similar thermal events at 573 °C which were endothermic and represented α to ß phase transition of quartz [25].

Microstructure observation of geopolymer stones

The optical images of samples GP04 (with foam) and GP02 (without foam) are shown in Fig. 6. The texture and packing arrangement of the stones in the samples are noticed completely different which may affect their strength and porosity. The high resolution (16MP) camera was used to acquire the

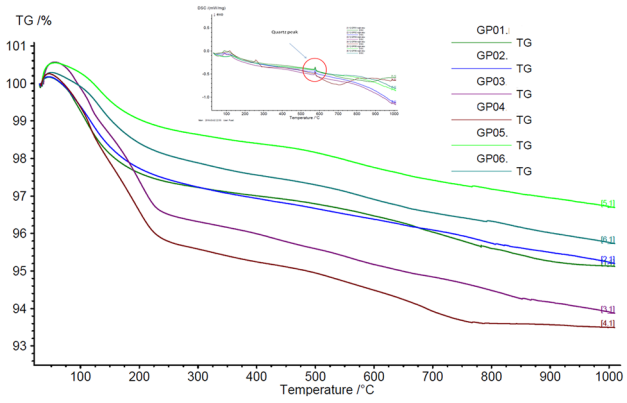

Fig. 5 TG curves of the geopolymer stones. DSC curves are also shown in the insertion

Table 6 The types of released water during heat treatment (from Fig. 5) [11]

Samples	Physically bonded water (0–100 °C) (wt.%)	Chemically bonded water (101–300 °C) (wt.%)	Dehydration of OH groups and polycondensation into siloxo bond Si–O–Si. (301°–1000°) (wt.%)
GP01	1.28	1.87	2.09
GP02	1.27	2.02	2.00
GP03	1.60	3.42	2.08
GP04	1.88	3.62	2.40
GP05	0.95	1.58	1.92
GP06	1.14	1.96	2.12

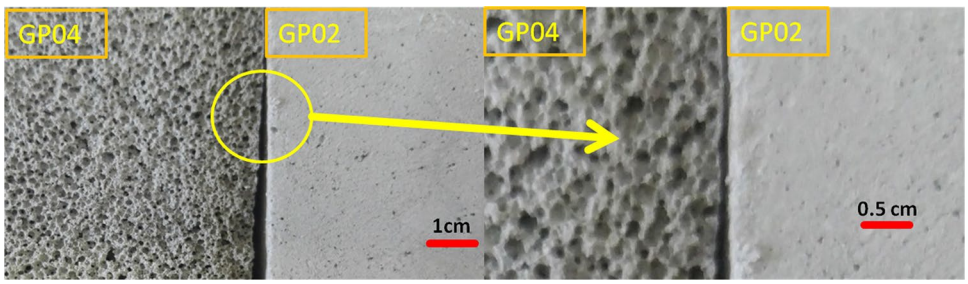

Fig. 6 High resolution optical images of GP02 and GP04

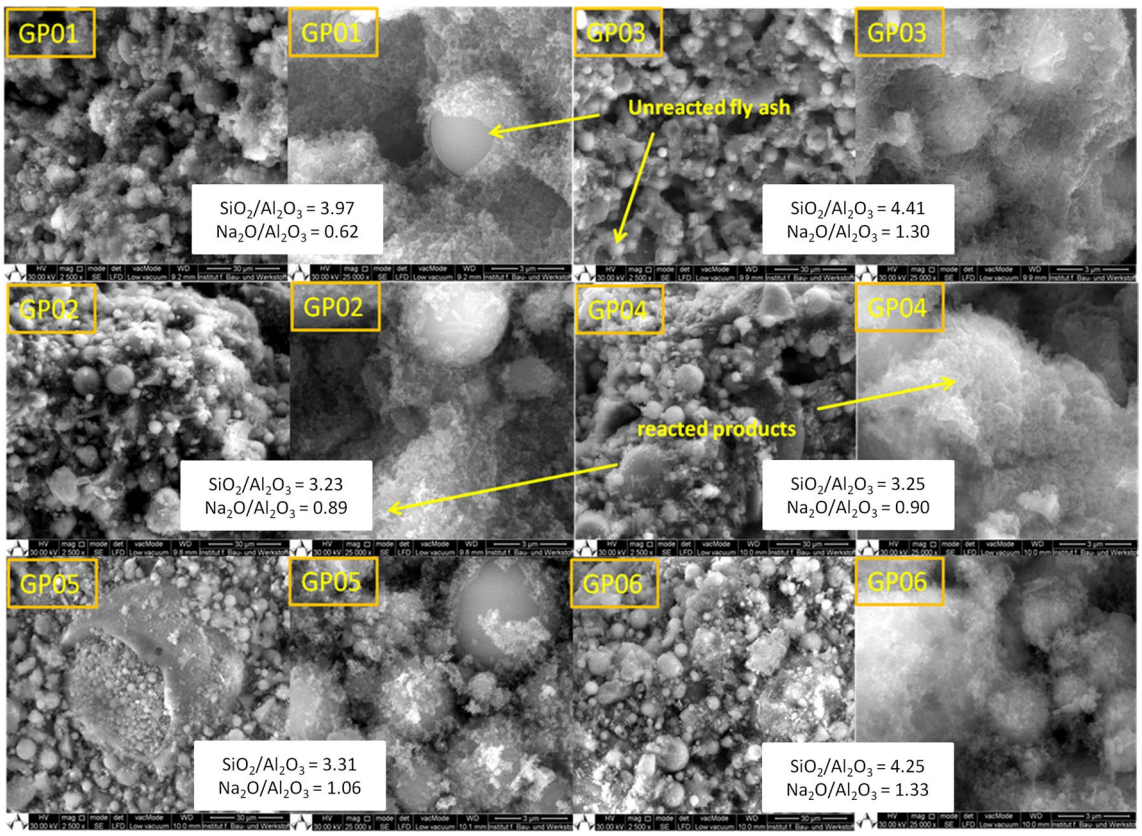

Fig. 7 SEM images of the geopolymer stones

images. The appearance of the nearly homogeneous pore structure of the foamed sample was compared to the solid geopolymer stone. Similar trends were found in the case of other pairs (GP01 and GP03 and GP05 and GP06).

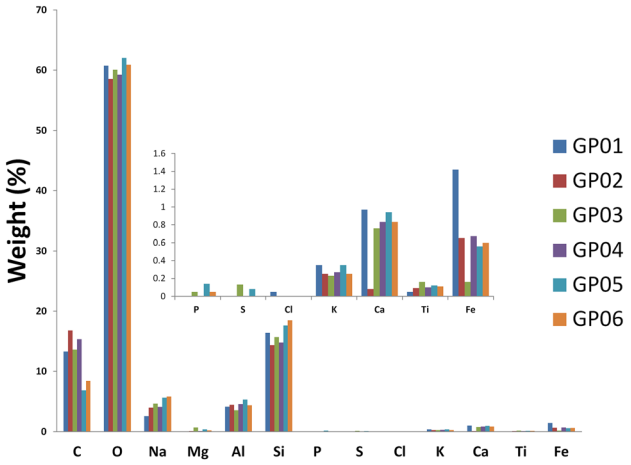

Fig. 8 EDX analytical composition of the geopolymer stones

The microstructure and corresponding elemental composition from a selected region in each sample were examined using the SEM equipment. The geopolymer concretes without foam (GP01, GP02, and GP05) are shown in Fig. 7 (left) which have a denser (see Fig. 1) matrix compared to the samples with foam (GP03, GP04, and GP06) (Fig. 7 right). Both types of samples were containing unreacted spherical vitreous particles of fly ash and also some incomplete reaction of the fly ash. The gel structure was limited to a few sections of the concrete compared to the lightweight alternatives which have several pores as shown in Fig. 7. The foamed concretes have a high variety of cracks and a pool of unreacted fly ash in their structure compared to the samples without foam. This feature without foamed samples might be responsible for the rigid structure (less porous) and higher mechanical strength obtained from the strength test (see Fig. 1).

The comparison of EDX results for the 6 samples is shown in Fig. 8. The sodium content was found to be higher in with foamed concrete samples compared to corresponding without foam samples (GP01and GP03, GP02, and GP04, GP05 and GP06) in point analysis by EDX. On the other hand, the aluminum content showed relatively lower in the foamed concretes pairs with respect to without foam concretes pair.

The physical and mechanical properties of geopolymers were a function of the SiO_2/Al_2O_3 and Na_2O/Al_2O_3 ratios [26]. The addition of waste water and used sand played (GP02 and GP04) a role in the attack of alumino-silicate material leading to lower values of SiO_2/Al_2O_3 and but in case of Na_2O/Al_2O_3 ratios shown no trend which was comparable (see Figs. 7 and 8).

They might be a possibility of higher Al related reaction products in geopolymer concretes compared to geopolymer

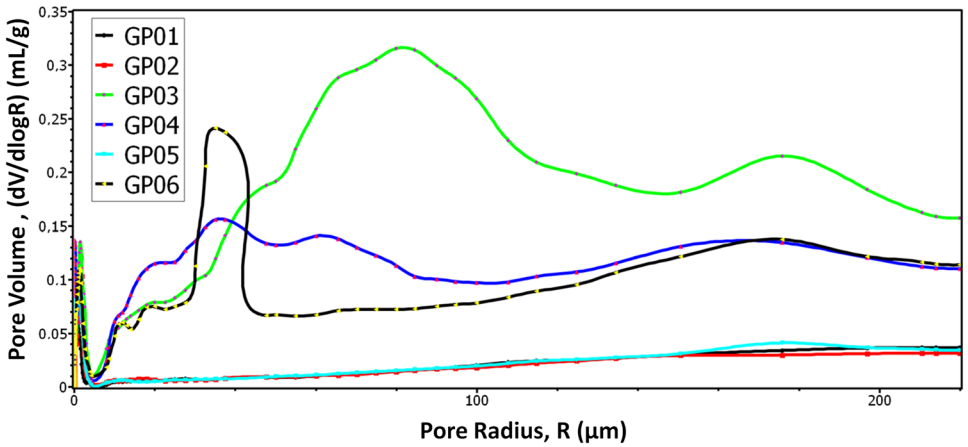

Fig. 9 Pore size distributions of the geopolymer stones by MIP

Table 7 Pore characteristics of prepared samples via MIP

Sample name	Bulk density (g/ml)	True density (g/ml)	Porosity (vol.%)	Pore area (10–220 µm) (vol.%)	Pore area (0.03–10 µm) (vol.%)	Pore area (0.002–0.03 µm) (vol.%)
GP01	1.78	2.53	29.59	3.32	23.79	2.48
GP02	1.86	2.51	25.68	3.36	20.93	1.40
GP03	1.27	2.29	44.41	27.91	15.88	0.62
GP04	1.30	2.29	42.85	20.61	22.09	0.15
GP05	1.80	2.52	28.51	3.45	23.20	1.86
GP06	1.47	2.38	38.35	18.87	18.89	0.59

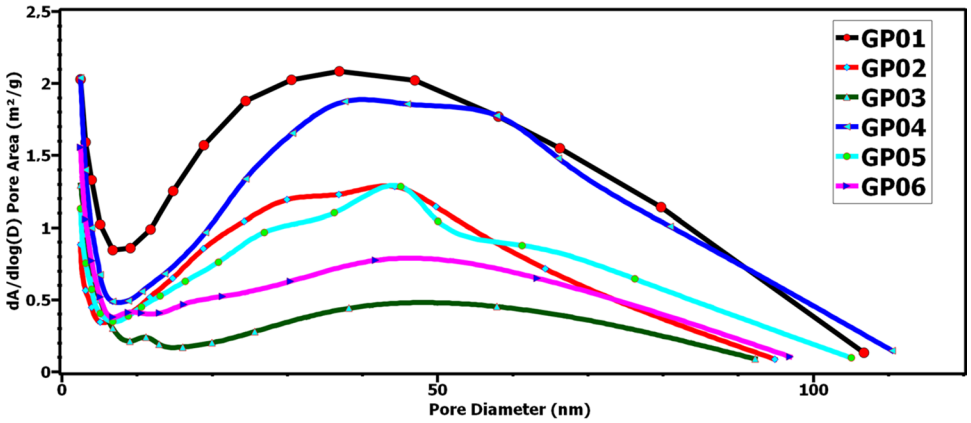

Fig. 10 Pore size distribution of the geopolymer stones by gas adsorption (N_2)

foamed concretes. Furthermore, GP02 and GP04 stone have lower Si and O contents compared to GP05 and GP06 for the respective point analyses.

The smaller pores were found in geopolymer concretes without foam, while the foamed geopolymer concretes also showed larger pore distributions. Figure 9 illustrates the pore size distribution of each geopolymer concrete. All foamed geopolymer concrete samples had higher porosity compared (see Table 7) to geopolymer concrete samples without foam as it was expected to fulfill the aim of generating foam geopolymer like insulating materials. The GP03 has the highest porosity volume of 44.41 vol.% followed by GP04 with 42.85 vol.%. The least porosity was found in the geopolymer concrete stone without foam obtained from waste water and used sand (GP02, 25.59 vol.%). A correlation between density and porosity of each concretes were found according to revealed result by MIP. A higher density and lower pore volume (see Table 7) of the geopolymer were found for concretes (GP02, with a little amount of higher packing density) made with waste water and used sand in comparison to concrete (GP05) prepared with tap water and new sand.

The pore size distribution in the range from 1.7 to 100 nm of these samples was evaluated by BJH desorption analysis. Figure 10 shows the pore size distribution of each geopolymer concrete. It should be addressed the adsorption isotherms were checked to ensure the false peak caused by N_2 condensation can be eliminated from the measurements. The Fig. 10 shows no clear indication of foam concrete samples of pore area distribution like MIP investigations (see Fig. 9).

The N_2 gas adsorption analysis showed the highest specific surface area (S_{BET}) (3.2 m^2/g) for GP01 compared to other samples (1.6, 0.9, 2.1, 1.4, and 1.3 m^2/g from GP02 to GP06 respectively). However, the total pore volume was not showing any relation (see Table 8). This result is an indication of more pores in the matrix.

The GP02 concrete had a lower surface area compared to its corresponding foamed concrete (GP04). A slightly higher surface area was found in GP05 in respect to its foamed concrete (GP06). It is worthy to note that the specific surface area found for GP01 concrete was unexpectedly higher compared to its corresponding foam concrete (GP03). However, GP03, GP04, and GP06 concrete have a greater pore volume compared to other geopolymer concretes. This result is in agreement with the density and porosity obtained from MIP and SEM.

Strength observation of geopolymer stones

The calculated bulk density, compressive and flexural strength found for each of the geopolymer stones are shown in Fig. 11. GP02 had the highest compressive and flexural strength of 17.25 and 6.50 N/mm^2 respectively. The foam geopolymer concrete with waste water (GP04) also showed higher compressive and flexural strengths compared to the samples made with tap water (GP03 and GP06). However; GP05 geopolymer concrete stone with fresh sand also showed a similar compressive and flexural strength with tap water and used sand geopolymer concrete (GP01) compare to geopolymer concrete stone with used sand and waste water (GP02).

Table 8 Specific surface area (S_{BET}) and pore characteristics of prepared samples via N_2 gas adsorption

Samples	S_{BET} (m^2/g)	Pore size[a] (nm)	Pore volume[b] (cm^3/g)
GP01	3.18	26.61	0.015
GP02	1.56	27.54	0.007
GP03	0.93	20.44	0.003
GP04	2.08	29.45	0.014
GP05	1.36	28.01	0.008
GP06	1.30	22.79	0.006

[a]BJH desorption average pore diameter

[b]BJH desorption cumulative volume of pores

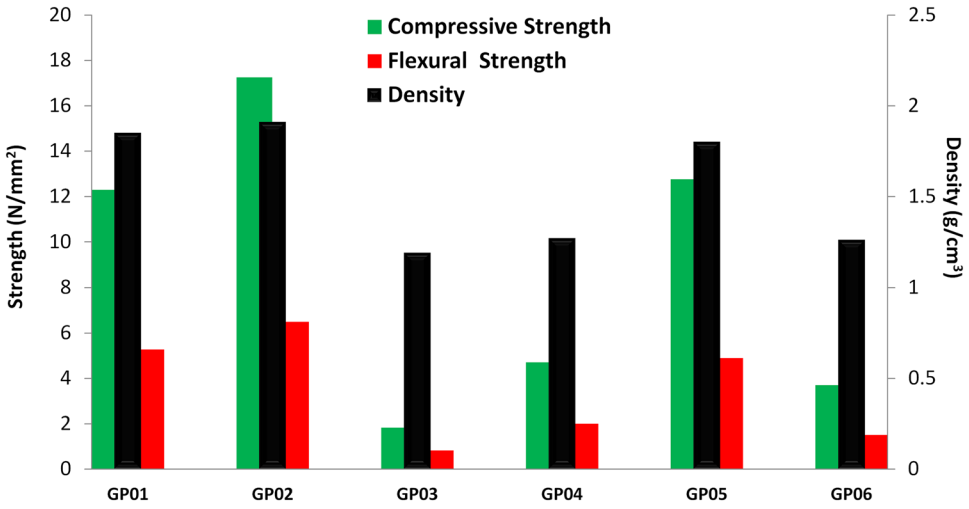

Fig. 11 Mechanical strengths of the geopolymer concretes and geopolymer foam concretes after curing for 6 days

Conclusion

This study describes the use of industrial by-products, waste water and fly ash as raw materials for the preparation of geopolymers which exhibit better properties and could serve as an alternative to conventional cement-based concrete. The product itself has very good properties such as good strength and low porosity. The foam geopolymers could be a potential substitute for conventional insulating materials. By the use of these materials, a sustainable concrete with good technical properties will be obtained.

The following conclusions can be drawn on the base of the experimental findings of this study:

1. The direct utilization of high alkaline waste water in the geopolymer system avoids treatment cost and environmental impact.
2. An improvement in the mechanical properties of fly ash-based geopolymers was observed for the samples made with waste water compared to tap water (see Fig. 11).
3. The obtained results showed that waste water made geopolymer concretes (GP02) have relatively lower pore volume (improved packing density) compared to the geopolymer concretes made with tap water (GP01 and GP05).

Open Access This article is licensed under a Creative Commons Attribution 4.0 International License, which permits use, sharing, adaptation, distribution and reproduction in any medium or format, as long as you give appropriate credit to the original author(s) and the source, provide a link to the Creative Commons licence, and indicate if changes were made. The images or other third party material in this article are included in the article's Creative Commons licence, unless indicated otherwise in a credit line to the material. If material is not included in the article's Creative Commons licence and your intended use is not permitted by statutory regulation or exceeds the permitted use, you will need to obtain permission directly from the copyright holder. To view a copy of this licence, visit http://creativecommons.org/licenses/by/4.0/.

References

1. Schneider M, Romer M, Tschudin M, Bolio H (2011) Sustainable cement production—present and future. Cem Concr Res 41:642–650
2. Davidovits J (1994) Geopolymer cements to minimize carbon-dioxide green house warming. World Resour Rev 6(2):263–278
3. Yang K-H, Song J-K, Song K-I (2013) Assessment of CO2 reduction of alkali-activated concrete. J Clean Prod 39:265–272
4. McCaffrey R (2002) Climate change and the cement industry, global cement and lime magazine. Environmental Special Issue, pp 15–19
5. Duxson P (2007) Geopolymer technology: the current state of the art. J Mater Sci 42:2917–2933
6. McLellan BC, Williams RP, Lay J, Van Riessen A, Corder GD (2011) Costs and carbon emissions for geopolymer pastes in comparison to ordinary Portland cement. J Clean Prod 19:1080–1090
7. Duxson P, Provis JL, Lukey GC, Van Deventer JSJ (2007) The role of inorganic polymer technology in the development of 'green concrete'. Cem Concr Res 37:1590–1597
8. Mehta A, Siddique R (2017) Strength, permeability and microstructural characteristics of low-calcium fly ash based geopolymers. Constr Build Mater 141:325–334
9. Sathonsaowaphak A, Chindaprasirt P, Pimraksa K (2009) Workability and strength of lignite bottom ash geopolymer mortar. J Hazard Mater 168:44–50
10. Rangan BV (2007) Design, properties, and applications of low-calcium fly ash-based geopolymer concrete developments in porous, biological and geopolymer ceramics: ceramic engineering and science proceedings, vol 28, no 9. Wiley, New York
11. Davidovits J (2015) Geopolymer chemistry and applications, 4th edn **(ISBN: 9782951482098)**
12. Part WK, Ramli M, Cheah CB (2015) An overview on the influence of various factors on the properties of geopolymer

concrete derived from industrial by-products. Constr Build Mater 77:370–395
13. Bakria AMMA (2011) The effect of curing temperature on physical and chemical properties of geopolymers. Phys Procedia 22:286–291
14. Rangan BV (2005) Low-calcium fly-ash-based geopolymer concrete, research report GC 1, Faculty of Engineering, Curtin University of Technology, Perth, Australia
15. Kong DLY, Sanjayan JG (2008) Damage behavior of geopolymer composites exposed to elevated temperatures. Cement Concr Compos 30:986–991
16. Duxson P (2005) Understanding the relationship between geopolymer composition, microstructure and mechanical properties. Colloids Surf A 269:47–58
17. Bakharev T (2005) Resistance of geopolymer materials to acid attack. Cem Concr Res 35:658–670
18. Guney Y, Sari YD, Yalcin M, Tuncan A, Donmez S (2010) Reusage of waste foundry sand in high-strength concrete. Waste Manage 30:1705–1713
19. Siddique R, Gde S, Noumowe A (2009) Effect of used-foundry sand on the mechanical properties of concrete. Constr Build Mater 23:976–980
20. Hardjito D, Wallah SE, Sumajouw DMJ, Rangan BV (2004) On the development of fly ash-based geopolymer concrete. Mater J 101(6):467–472
21. Abdullah MMAB (2012) Fly ash-based geopolymer lightweight concrete using foaming agent. Int J Mol Sci 13:7186–7198
22. Chindaprasirt P, Somna K, Jaturapitakkul C, Kajitvichyanukul P (2011) NaOH-activated ground fly ash geopolymer cured at ambient temperature. Fuel 90:2118–2124
23. Fernández-Jiménez APA (2005) Mid-infrared spectroscopic studies of alkali-activated fly ash. Microporous Mesoporous Mater 86(1–3):207–214
24. Fernández-Jiménez APA, Pastor JY, Martín A (2008) New Cementitious materials based on alkali-activated fly ash: performance at high temperatures. J Am Ceram Soc 91(10):3308–3314
25. Peng Z, Redfern SAT (2013) Mechanical properties of quartz at the α-ß phase transition: implications for tectonic and seismic anomalies. Geochem Geophys Geosyst 14:18–28
26. Davidovits J (1991) Geopolymers: inorganic polymeric newmaterials. J Therm Anal 37:1633–1656

Publisher's Note Springer Nature remains neutral with regard to jurisdictional claims in published maps and institutional affiliations.